

# J80-187

## Modeling Nonlinear Deformation of Carbon-Carbon Composite Materials

80003  
80008

Robert M. Jones\*  
Southern Methodist University, Dallas, Tex.

Carbon-carbon composite materials have different nonlinear stress-strain behavior under tension loading than under compression loading. The Jones-Nelson-Morgan nonlinear multimodulus material model is fit to the characteristics of AVCO Mod 3a carbon-carbon, which consists of woven layers of orthogonal fibers in the  $x$ - $y$  plane pierced by fibers in the  $z$  direction. The model is thus defined by use of measured behavior in the principal material directions. Then, the model is validated by comparison of predicted and measured response under uniaxial off-axis loading in tension and in compression.

### Nomenclature

$A_i, B_i, C_i, U_{0i}$	= constants in $i$ th mechanical property equation, Eq. (1)
$E_x, E_y, E_z$	= Young's moduli in $x, y$ , and $z$ directions
$G_{xy}, G_{xz}$	= shear moduli in $x$ - $y$ and $x$ - $z$ planes
$U$	= strain energy density
$x, y, z$	= rectangular coordinates in principal material directions
$\nu_{xy(xz)}$	= Poisson's ratio for contraction in the $y$ ( $z$ ) direction because of extension in the $x$ direction

### Superscripts

45	= 45 deg to $x$ direction
( )*	= special values defined in Figs. 1 and 2

### Subscripts

$c$	= compression
$t$	= tension
$xy(xz)$	= $x$ - $y$ ( $x$ - $z$ ) plane

### Introduction

**C**ARBON-CARBON composite materials are composed of carbon fibers arranged in two or more directions in a carbon matrix. Thus, carbon-carbon is not a single material, but a broad class of materials. Many types of carbon-carbon are manufactured including various kinds of woven fibers or felt materials, both of which are coated or impregnated with a matrix material in a vapor deposition or a pressure impregnation process. The combination of materials is subsequently carbonized and graphitized to create carbon-carbon.

Because of the high-temperature processing necessary to manufacture carbon-carbon materials, they are used in elevated temperature applications such as re-entry vehicle nosetips and rocket nozzles where structural integrity is essential. Both nosetips and nozzles are subjected to severe environments and require accurate design analysis to function. However, carbon-carbon materials have nonlinear stress-strain behavior under tension loading that is different from behavior under compression loading. Thus, proper

representation of actual material behavior is not possible in present design analysis methods.

The objective of this paper is to develop or adapt a nonlinear multimodulus model for carbon-carbon composite materials and to validate that model by comparison of predicted and measured response under generally precise laboratory conditions of uniaxial off-axis loading. The specific material addressed is AVCO Mod 3a carbon-carbon, which has a woven layer of orthogonal fibers in the  $x$ - $y$  plane and is pierced with fibers in the  $z$  direction. This material has perhaps been superseded in applications importance by several other carbon-carbons, but remains the *only* carbon-carbon for which sufficient experimental data exist to *validate* any material model. The material model developed is the Jones-Nelson-Morgan nonlinear multimodulus model which is validated for ATJ-S graphite<sup>1,2</sup> as well as boron-epoxy and graphite-epoxy.<sup>3</sup> However, for carbon-carbon, additional interpretation of the model must be made. The material model is validated by comparing predicted and measured strain response to uniaxial loading applied at an angle to a fiber direction in either the  $x$ - $y$  plane or the  $x$ - $z$  plane in addition to shear response. Material models could be developed for other carbon-carbon materials, but none could be validated because essential off-axis tests have not been performed. Nevertheless, AVCO Mod 3a is a representative member of the important class of three-dimensional orthogonally pierced and woven fabric carbon-carbon materials. Hence, construction and validation of a Mod 3a model should be a useful guide for modeling this entire class of composite materials.

### Carbon-Carbon Nonlinear Multimodulus Material Model

The carbon-carbon material modeled in this paper is AVCO Mod 3a, a rectangularly orthotropic material constructed of woven fibers in the  $x$ - $y$  plane with pierced fibers in the  $z$  direction. An equal number of fibers exists in the  $x$  direction as in the  $y$  direction on the average because the woven layers in the  $x$ - $y$  plane are laid down with the warp and fill directions alternating from layer to layer. The mechanical behavior of Mod 3a is reported by Starrett, Weiler, and Pears<sup>4</sup> for room temperature and several elevated temperatures. The behavior at room temperature will be addressed because it appears to involve more consistent data than exist at elevated temperatures. Other carbon-carbon materials could be modeled, but stress-strain curves essential to the validation of those models are not available. Thus, AVCO Mod 3a is the *only* carbon-carbon material which we can both model and validate. The modeling with the Jones-Nelson-Morgan model

Presented as Paper 79-0774 at the AIAA/ASME/ASCE/AHS 20th Structures, Structural Dynamics, and Materials Conference, St. Louis, Mo., April 4-6, 1979; received Feb. 2, 1979; revision received Feb. 21, 1980. Copyright © 1979 by R. M. Jones. Published by the American Institute of Aeronautics and Astronautics, Inc., with permission.

Index categories: Structural Statics; Structural Composite Materials.

\*Professor of Solid Mechanics, Civil and Mechanical Engineering Dept. Associate Fellow AIAA.

will be described in this section, and the model validation will be addressed in the next two sections.

The Jones-Nelson-Morgan nonlinear multimodulus material model is basically an expression of the secant moduli of a material as a function of strain energy density in the form

$$\text{Mechanical property}_i = A_i \left[ 1 - B_i \left( \frac{U}{U_{0i}} \right)^{C_i} \right] \quad (1)$$

where the strain energy density (hereafter abbreviated as strain energy) is:

$$U = (\sigma_x \epsilon_x + \sigma_y \epsilon_y + \sigma_z \epsilon_z + \tau_{yz} \gamma_{yz} + \tau_{zx} \gamma_{zx} + \tau_{xy} \gamma_{xy}) / 2 \quad (2)$$

and the constants  $A_i$ ,  $B_i$ , and  $C_i$  are the initial values of the mechanical property, the initial curvature of the stress-strain curve, and the rate of change of curvature of the stress-strain curve, respectively. The subscript  $i$  in Eq. (1) is used to distinguish which mechanical property is addressed, and  $U_{0i}$  is used to nondimensionalize the bracketed term in Eq. (1).

The specific mechanical properties which must be modeled for AVCO Mod 3a are  $E_x$ ,  $E_z$ ,  $\nu_{xz}$ ,  $\nu_{xy}$ ,  $E_{xz}^{45}$ ,  $E_{xy}^{45}$  in both tension and compression. The behavior in the  $x$  direction is identical to that in the  $y$  direction because of the way in which Mod 3a is made. The 45 deg off-axis properties are pure tension or pure compression properties instead of the inherently mixed tension and compression character of shear behavior. The transformations from principal material directions to principal stress directions in the Jones-Nelson-Morgan nonlinear multimodulus material model take place with either tension or compression properties. A "tension shear modulus" (i.e., for use in transformations of tension mechanical properties) is back-calculated from the other properties with a relation of the form

$$1/G_{xz_t} = 4/E_{xz_t}^{45} - (1/E_{x_t} + 1/E_{z_t} - 2\nu_{xz_t}/E_{x_t}) \quad (3)$$

Similar relations exist for  $G_{xy_t}$ ,  $G_{xz_c}$ , and  $G_{xy_c}$ . However, these tension and compression shear moduli do not exist, i.e., they cannot be measured. They are only an artifice in the multimodulus formulation. The real (measurable) moduli  $G_{xy}$  and  $G_{xz}$  are the average of  $G_{xy_t}$  and  $G_{xy_c}$  plus  $G_{xz_t}$  and  $G_{xz_c}$ , respectively.

The constants  $A$ ,  $B$ , and  $C$  are determined from measured stress-strain data, which are converted to mechanical property vs strain energy data, as shown schematically in Fig. 1 by use of a nonlinear regression scheme developed by Jones and Morgan.<sup>3</sup> However, measured stress-strain data, and hence mechanical property vs strain energy data, do not exist for all strain energies corresponding to all possible multiaxial

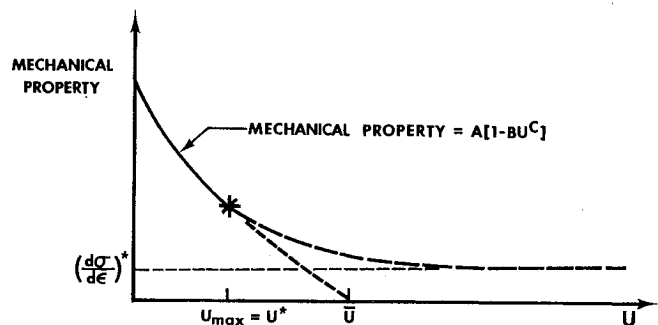


Fig. 1 Mechanical property vs strain energy curve extrapolation.

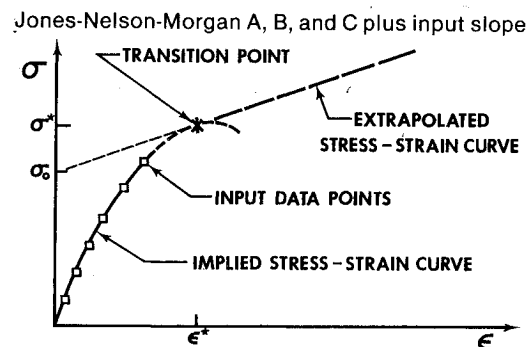


Fig. 2 Stress-strain curve extrapolation.

loading conditions (recall that mechanical properties are usually measured in uniaxial loading states). Thus, the mechanical property expression in Eq. (1) is valid only up to the last measured value of strain energy, i.e., up to strain energy  $U^*$  in Fig. 1. Above that strain energy, the measured stress-strain data must be extrapolated so that the mechanical properties are defined nonzero quantities for all values of strain energy.

In the Jones-Nelson-Morgan model, the stress-strain data are extrapolated by adding a linear extension to the implied stress-strain curve corresponding to the mechanical property expression in Eq. (1) as shown in Fig. 2. That is, for strains less than  $\epsilon^*$  in Fig. 2, the stress-strain data are approximated with Eq. (1), and for strains greater than  $\epsilon^*$ , the stress-strain behavior is extended as the straight line with slope  $E^*$ . The portion of the mechanical property vs strain energy curve to the right of  $U^*$  in Fig. 1 corresponds to the linear extension of the stress-strain curve data in Fig. 2. This extrapolation of the mechanical property vs strain energy data approaches a constant nonzero value as the strain energy increases. For carbon-carbon, the linear extension of the stress-strain curve

Table 1 Jones-Nelson-Morgan material model constants for AVCO Mod 3a carbon-carbon

Mechanical property <sup>a</sup>	$A^b$ , $10^6$ psi (GN/m <sup>2</sup> )	$B$	$C$	$U^*$ , psi ( $\mu$ N/m <sup>2</sup> )	$E^*$ , $10^6$ psi (GN/m <sup>2</sup> )	$\sigma_0$ , psi (MN/m <sup>2</sup> )
$E_{x_t}$	1.70(11.7)	0.197	0.341	31.1(214)	0.159(1.10)	4620(31.9)
$E_{z_t}$	13.4(92.4)	0.713	0.121	26.4(182)	3.25(22.4)	904(6.23)
$\nu_{xz_t}$	0.05	0	1	0	0	0
$\nu_{xy_t}$	0.11	0	1	0	0	0
$E_{xz_t}^{45}$	1.26(8.69)	0.268	0.619	3.86(26.6)	0	1930(13.3)
$E_{xy_t}^{45}$	1.44(9.93)	0.162	0.583	9.66(66.6)	0.0300(0.207)	3130(21.6)
$E_{x_c}$	1.49(10.3)	0.0721	0.457	57.8(399)	0.351(2.42)	5430(37.4)
$E_{z_c}$	2.40(16.5)	0.0316	0.907	6.86(47.3)	0.184(1.27)	4700(32.4)
$\nu_{xz_c}$	0.05	0	1	0	0	0
$\nu_{xy_c}$	0.11	0	1	0	0	0
$E_{xz_c}^{45}$	0.801(5.52)	0.169	0.462	15.8(109)	0.0541(0.373)	2620(18.1)
$E_{xy_c}^{45}$	1.35(9.31)	0.0505	0.795	20.5(141)	0	4950(34.1)

<sup>a</sup> The value of  $U_0$  is 1 psi (6.895  $\mu$ N/m<sup>2</sup>). <sup>b</sup> Poisson's ratios are dimensionless.

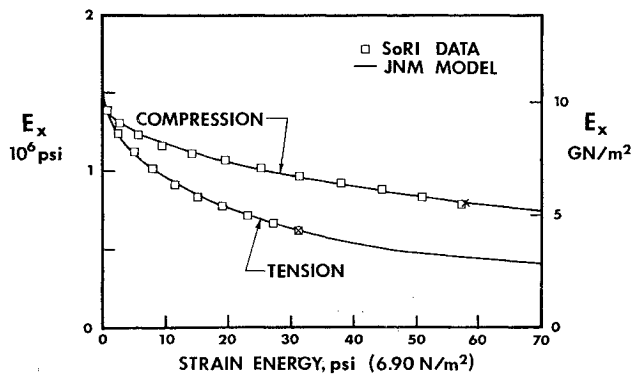
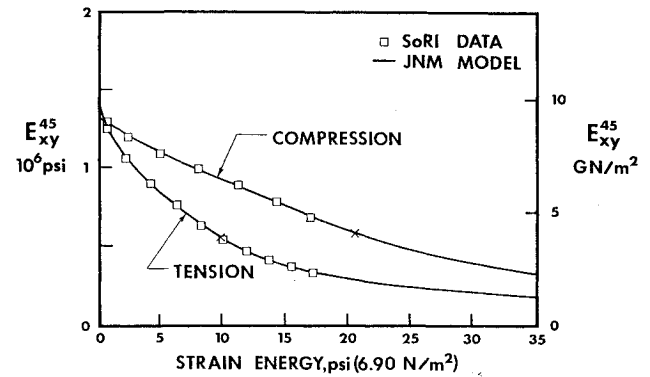
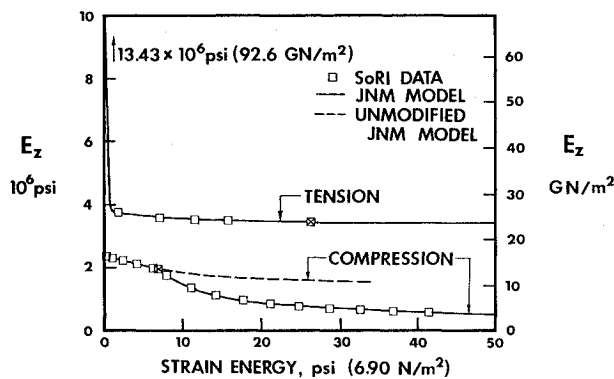
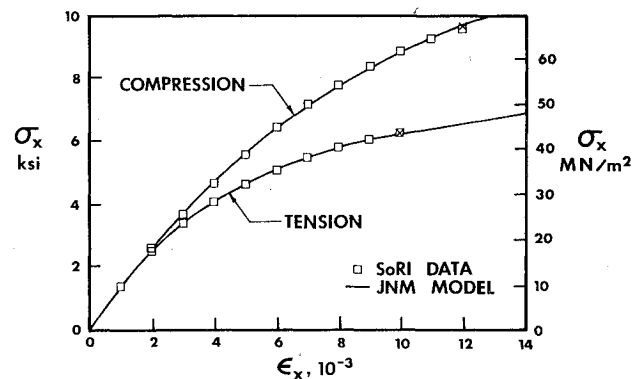
Fig. 3  $E_x$  vs strain energy.Fig. 6  $E_{xy}^{45}$  vs strain energy.Fig. 4  $E_z$  vs strain energy.

Fig. 7 Stress-strain behavior in the x direction.

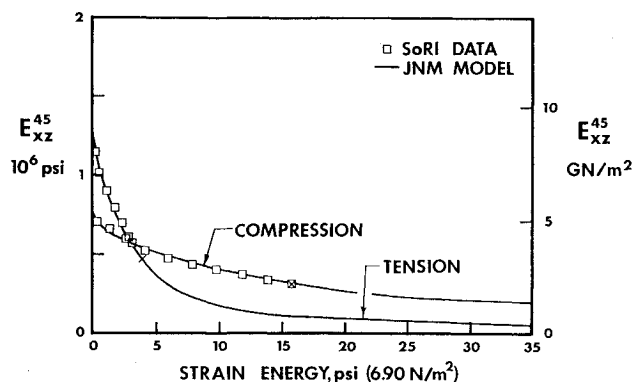
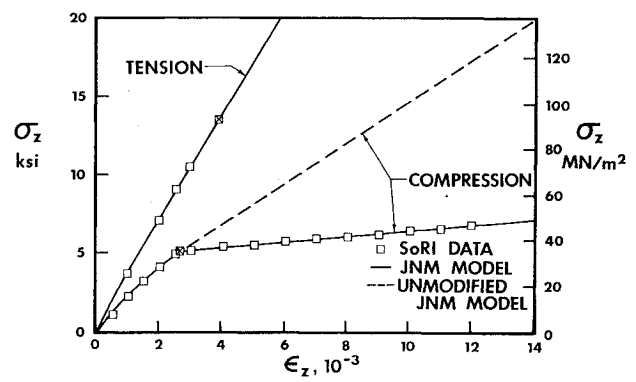
Fig. 5  $E_{xz}^{45}$  vs strain energy.

Fig. 8 Stress-strain behavior in the z direction.

is necessary to fit the measured data directly (without extrapolation); that is, the shape of many carbon-carbon stress-strain curves is quite similar to Fig. 2.

The numerical values for the Jones-Nelson-Morgan model for room temperature behavior of AVCO Mod 3a carbon-carbon are obtained with the JNM DATA program<sup>5</sup> and are given in Table 1. The mechanical property vs strain energy curves are displayed in Figs. 3-6, and the stress-strain curves are shown in Figs. 7-10. Note the significantly different behavior in tension than in compression. This type of behavior is the primary motivation for the multimodulus aspect of the Jones-Nelson-Morgan model. The requirement for a nonlinear model is obvious. The stress-strain behavior in the x direction in Figs. 3 and 7 is modeled with Eq. (1) until the last data point, whereupon the slope at the last data point is used. The behavior in the z direction in tension in Figs. 4 and 8 is modeled the same, but in compression a straight line is used to model the actual behavior (the solid line in Figs. 4 and 8 instead of the dashed line). The slope and intercept of the straight line are hand calculated to fit the data rather than

being obtained automatically from the JNM DATA computer program. The compression behavior at 45 deg to the x direction in the xz plane in Figs. 5 and 9 is modeled with Eq. (1) until the last data point is reached, and then a straight line with the slope at the last data point is used. In tension in Figs. 5 and 9, the behavior in Eq. (1) is continued until a zero slope is reached, and then a horizontal straight line is used. The same approach is used for the compression behavior at 45 deg to the x direction in the xy plane in Figs. 6 and 10. For the tension behavior in Figs. 6 and 10, the straight line extension is used to fit the last five data points. All Jones-Nelson-Morgan model fits of the data are quite good, as can be seen in Figs. 4-10.

The Poisson's ratios data are not entirely satisfying. Starrett and Pears<sup>6</sup> report

$$\nu_{xy_c} = 0.11 \quad \nu_{xz_c} = 0.03 \quad \nu_{zx_c} = 0.05$$

and feel "that these values are adequate for both tension and compression." However,  $\nu_{xz}$  should be obtainable from the

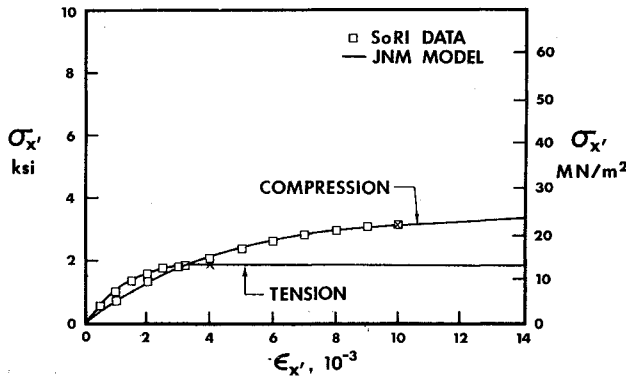


Fig. 9 Stress-strain behavior in the x-z plane at 45 deg to x axis.

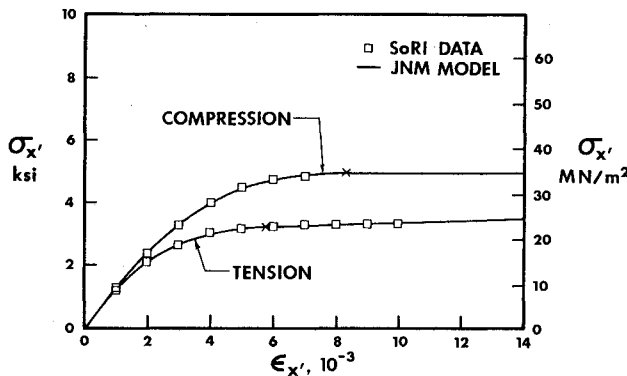


Fig. 10 Stress-strain behavior in the x-y plane at 45 deg to x axis.

reciprocal relation

$$\nu_{xz} = \nu_{zx} E_x / E_z$$

For compression properties,  $\nu_{xz}$  does turn out to be 0.03. However, for tension properties,  $\nu_{xz}$  is 0.02, or even as small as 0.006 if the values of  $A$  are used in the calculation. Moreover, Poisson's ratios are not reported to be a function of stress level, as would be expected for properties of a material with highly nonlinear stress-strain behavior. These are the reasons for some uneasiness about the values of Poisson's ratios in Table 1.

Data reported by Starrett, Weiler, and Pears<sup>4</sup> are in the form of "most probable value" curves to attempt to represent the amalgamation of many billets of Mod 3a carbon-carbon. That is, the billet-to-billet variation of mechanical properties is quite high. However, the most probable value curves are not sufficiently well-established on a statistical basis to render good comparisons between theory and experiment valid or to render unsatisfactory comparisons invalid. Accordingly, because of the discomforting nature of the Poisson's ratio data and the statistically unsatisfying nature of the other mechanical property data, complete confidence that a model has been established for AVCO Mod 3a carbon-carbon cannot be claimed. However, the quality of this model is higher than can be obtained for any other carbon-carbon because the data base for all other materials is even less satisfactory!

After the model is obtained, predictions of strains for specified multiaxial stress states can be made. However, the mechanical properties in Eq. (1) depend on the stresses and strains through the strain energy. Also, the stresses are related to the strains through the mechanical properties. Thus, for a given multiaxial loading condition, the stresses, strains, and mechanical properties are interdependent in transcendental relationships. Accordingly, the iteration procedure due to

Jones and Nelson<sup>1</sup> is used to find the correct stresses, strains, and mechanical properties for a given loading state.

### Effect of Shear Coupling on Uniaxial Off-Axis Loading

The strains for a specified uniform stress state can be predicted by use of the MULTIAX computer program, which is an implementation of the Jones-Nelson-Morgan nonlinear multimodulus material model for a uniform stress state (actually one element of a finite element program). However, actual test specimens under off-axis loading are in constrained states of strain, which do not coincide with the usual objective of a uniform state of strain and stress for a test specimen. The ends of a uniaxial test specimen are usually forced to remain parallel by clamping devices at each end. Thus, the shearing deformation that would otherwise develop is partially prevented, unless the observation is made at the center portion of a very long, slender test specimen. Pagano and Halpin<sup>7</sup> analyze the strains that exist in a simple rectangular tension (or compression) specimen of length  $L$  and width  $w$ . Their material behavior is linear elastic but orthotropic in principal material directions. However, the material behavior of present interest is nonlinear and orthotropic. Thus, their analysis must be modified or their results interpreted to account for the material nonlinearity. Then, the results of the new analysis for AVCO Mod 3a carbon-carbon will be examined.

For a rectangular specimen  $L$  long and  $w$  wide, Pagano and Halpin<sup>7</sup> obtain an apparent off-axis Young's modulus from their solution for the strains as

$$E_{x'}^* = \frac{\sigma_{x'}}{\epsilon_{y'}} = \left( \frac{1}{1-\eta} \right) \frac{1}{\bar{S}_{11}} \quad (4)$$

where

$$\eta = 3\bar{S}_{16}^2 / \{ \bar{S}_{11} [3\bar{S}_{66} + 2\bar{S}_{11} (L/w)^2] \} \quad (5)$$

$x'$  and  $y'$  are coordinates at angle  $\theta$  to the x-y coordinates as in Fig. 11, and the  $\bar{S}_{ij}$  are the transformed compliances of an orthotropic material (see Jones<sup>8</sup>). As  $L/w$  approaches infinity (a long, slender specimen),  $\eta$  approaches zero, so  $E_{x'}^*$  approaches  $E_{x'} = 1/\bar{S}_{11}$ , the Young's modulus in a uniform stress and strain state. On the other hand, as  $L/w$  approaches zero (a short, wide specimen),  $E_{x'}^*$  approaches

$$E_{x'}^* = \bar{S}_{66} / (\bar{S}_{11}\bar{S}_{66} - \bar{S}_{16}^2) \quad (6)$$

which can be shown to be less than  $\bar{Q}_{11}$ , the transformed reduced stiffness of an orthotropic material (see Jones<sup>8</sup>). For AVCO Mod 3a carbon-carbon,  $E_{x'}^*$  is well above the actual modulus  $E_{x'}$ , but not as much above as is  $\bar{Q}_{11}$ .

For a specific applied stress  $\sigma_{x'}$ , the implication of shear coupling for a specimen of length  $L$  and width  $w$  is that the axial strain  $\epsilon_{x'}$  is smaller than without shear coupling, and is obtained by multiplying the uniform stress and strain state by the factor  $(1-\eta)$ :

$$\epsilon_{x'}^{\text{actual}} = (1-\eta) \epsilon_{x'}^{\text{uniform}} \quad (7)$$

or, if the modulus factor is defined as  $1/(1-\eta)$ , then we divide the uniform stress and strain state strain by the modulus factor.

Similarly, Pagano and Halpin obtain the lateral and shear strains along the specimen centerline as

$$\epsilon_{y'} = \left[ \frac{3\bar{S}_{11}\bar{S}_{66} + 2\bar{S}_{11}^2 (L/w)^2 - 3\bar{S}_{11}\bar{S}_{16}\bar{S}_{26}/\bar{S}_{12}}{3(\bar{S}_{11}\bar{S}_{66} - \bar{S}_{16}^2) + 2\bar{S}_{11}^2 (L/w)^2} \right] \frac{\bar{S}_{12}}{\bar{S}_{11}} \epsilon_{x'} \quad (8)$$

$$\gamma_{x'y'} = \left\{ \left\{ \frac{1}{2} \left( \frac{w}{L} \right)^2 \left[ \frac{\bar{S}_{66}}{\bar{S}_{11}} - \left( \frac{\bar{S}_{16}}{\bar{S}_{11}} \right)^2 \right] + 1 \right\} \right\} \frac{\bar{S}_{16}}{\bar{S}_{11}} \epsilon_{x'} \quad (9)$$

For long, slender specimens ( $L/w \rightarrow \infty$ ), Eqs. (8) and (9) reduce to

$$\epsilon_{y'} = (\bar{S}_{12}/\bar{S}_{11})\epsilon_{x'} \quad (10)$$

$$\gamma_{x'y'} = (\bar{S}_{16}/\bar{S}_{11})\epsilon_{x'} \quad (11)$$

i.e., the uniform stress and strain state strains. However, for short, wide specimens ( $L/w \rightarrow 0$ ), Eqs. (8) and (9) reduce to

$$\epsilon_{y'} = \frac{\bar{S}_{12}\bar{S}_{66} - \bar{S}_{16}\bar{S}_{26}}{\bar{S}_{11}\bar{S}_{66} - \bar{S}_{16}^2}\epsilon_{x'} \quad (12)$$

$$\gamma_{x'y'} = 0 \quad (13)$$

which for the shear strain is the same as the simple solution for the short, wide specimen. However, for the transverse strain, Pagano and Halpin obtain larger values than for the simple solution. In fact, for AVCO Mod 3a carbon-carbon, the lateral strain is a substantial fraction (nearly  $\frac{3}{4}$ ) of the axial strain for off-axis angles near 60 deg. For actual specimens of length  $L$  and width  $w$ , the actual shear strain is always less than the uniform stress and strain state shear strain, and can be obtained by multiplying the uniform strain state strain by the double braced term in Eq. (9). Similarly, the actual transverse strain is obtained by multiplying the uniform strain state strain by the bracketed term in Eq. (8).

The key issue now is how the foregoing analysis can be used in the analysis of materials with nonlinear stress-strain behavior. The Pagano and Halpin analysis is adapted to treat nonlinear material behavior by using the compliances as a function of stress levels in all of the preceding equations. That is, secant moduli are used to calculate the compliances in a deformation theory of orthotropic plasticity (the Jones-Nelson-Morgan model). As the stress level increases in an off-axis test, the compliances grow larger and the moduli get smaller. Thus, the modulus reduction factors and strain reduction factors can be calculated for use in modifications of the MULTIAX strain predictions for off-axis loading.

The magnitudes by which the uniform strain state strains from MULTIAX must be adjusted to obtain reasonable approximations of actual test specimen behavior depend on many factors. These factors include the specimen length-to-width ratio, the strain under consideration, the loading level, the plane of the material being loaded, and the off-axis loading angle  $\theta$ . For example, the normal strains are decreased such that the apparent modulus exceeds the actual modulus by up to 30%, as in Fig. 11, for compression loading of 3000 psi ( $20.7 \text{ MN/m}^2$ ) in the  $x$ - $z$  plane. For a test specimen geometry of  $L/w = 4$ , the correction to the normal strain is about 5% at  $\theta = 25$  deg and 10% at  $\theta = 70$  deg. The shear strain reduction factor  $\gamma_{R_{XZ}}$  for off-axis compression loading in the  $x$ - $z$  plane

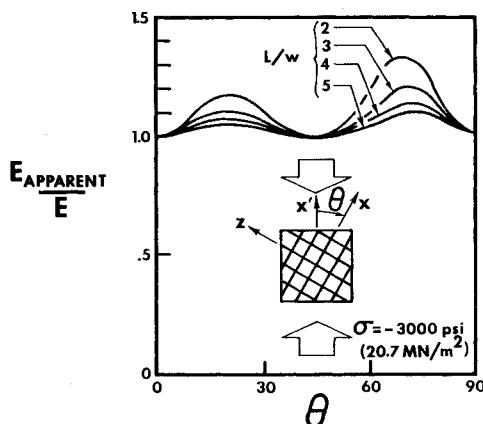


Fig. 11 Effective compression modulus increase under off-axis loading in  $x$ - $z$  plane.

is shown as a function of off-axis angle and specimen length-to-width ratio for a specific compression stress in Fig. 12. There, the reduction factor is about 20% for  $\theta = 25$  deg and  $\theta = 70$  deg if  $L/w = 4$ . The reductions in tension in the  $x$ - $z$  plane are slightly less than those in compression and even less in the  $x$ - $y$  plane. More comprehensive and specific results are presented by Jones.<sup>9</sup> This type of strain adjustment is performed to predict the strain response in the next section.

### Comparison of Predicted and Measured Strain Response for Uniaxial Off-Axis Loading of AVCO Mod 3a Carbon-Carbon

Starrett, Weiler, and Pears<sup>4</sup> subjected specimens of AVCO Mod 3a carbon-carbon to uniaxial tension and compression off-axis loading in the  $x$ - $y$  and  $x$ - $z$  planes. Their specimens have length-to-width ratios of approximately four and five (approximate because of specimen fillets). The Jones-Nelson-Morgan nonlinear multimodulus material model is used in the MULTIAX computer program to predict uniform strain state strains under the off-axis loading applied to the test specimens. Also in the MULTIAX program are strain

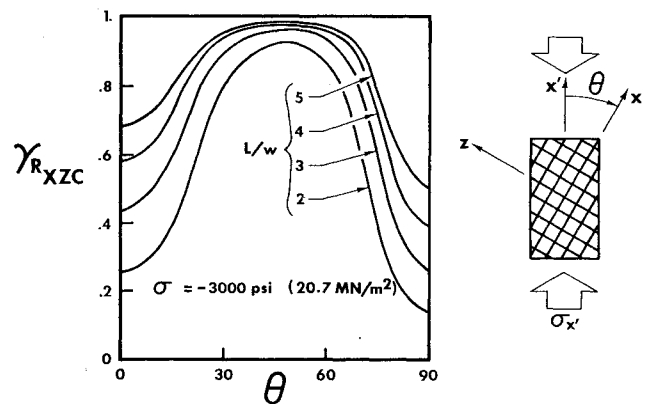


Fig. 12 Shear strain reduction factor for off-axis compression loading in  $x$ - $z$  plane.

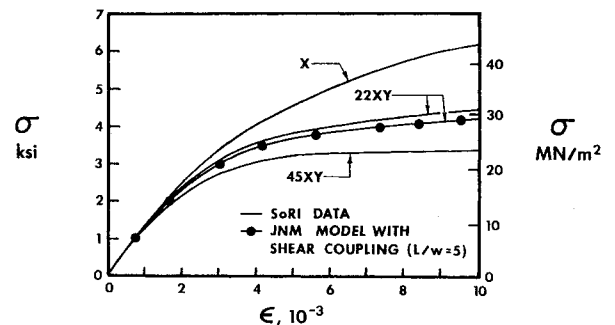


Fig. 13 Tension stress-strain behavior in  $x$ - $y$  plane.

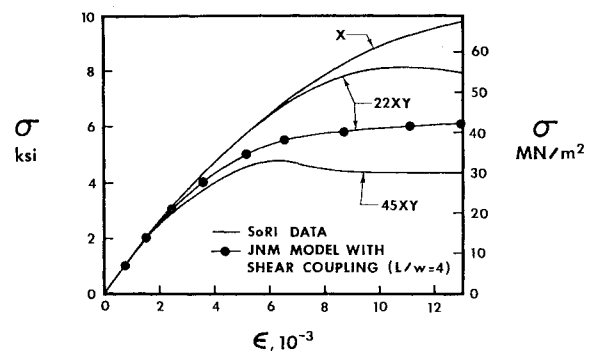


Fig. 14 Compression stress-strain behavior in  $x$ - $y$  plane.

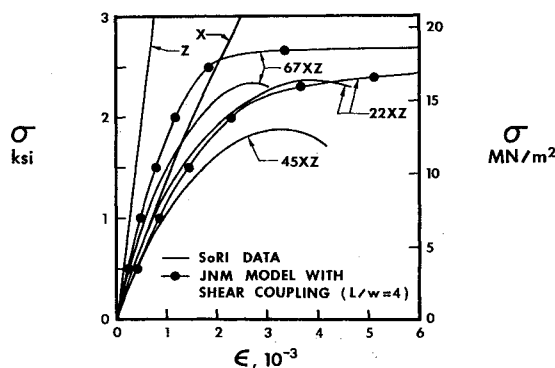


Fig. 15 Tension stress-strain behavior in x-z plane.

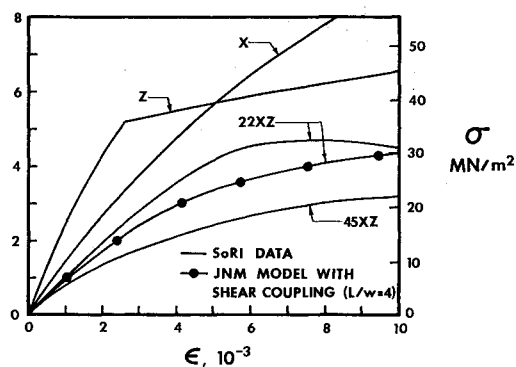


Fig. 16 Compression stress-strain behavior in x-z plane.

corrections caused by shear coupling for the length-to-width ratios of the actual test specimens as described in the preceding section.

Following are the predicted and measured strain response for these specimens used to validate the Jones-Nelson-Morgan material model. Generally, the uniaxial loading is applied at 22½ deg to the x direction in the x-y plane and in the x-z plane. In only one case is response at 67½ deg to the x direction measured. Shear loading is also applied, and the results are used as another *independent* validation of the Jones-Nelson-Morgan model predictions. The word *independent* is used because no shear behavior is used to define or construct the Jones-Nelson-Morgan model.

The x-y plane tension stress-strain behavior is shown in Fig. 13, where the x direction behavior, identical to the y direction behavior, is displayed along with the behavior at 45 deg to the x direction (the 45xy curve). Those two curves are part of the behavior used to define the Jones-Nelson-Morgan material model. The model is used to predict the response at 22½ deg to the x direction, which is very close to the measured response. A similar set of curves is shown for the x-y plane compression behavior in Fig. 14. However, the Jones-Nelson-Morgan model is not forced to dip as low as the actual 45xy curve does. Even so, the predicted response at 22½ deg is well below the measured response. However, the measured response looks quite high in that it seems to be too close to the x direction behavior and not close enough to the behavior at 45 deg to the x direction.

The x-z plane tension behavior is shown in Fig. 15, where the x direction behavior, z direction behavior, and the behavior at 45 deg to the x direction (the 45xz curve) are displayed. Those three curves are part of the behavior used to define the Jones-Nelson-Morgan material model. The model is used to predict the response at 22½ and 67½ deg to the x direction. The predicted response at 22½ deg, the 22xz curve is quite close to the measured behavior. On the other hand, the predicted response at 67½ deg, the 67xz curve, is above the measured behavior. However, the measured 67½ deg response appears a bit low, i.e., it would seem reasonable for

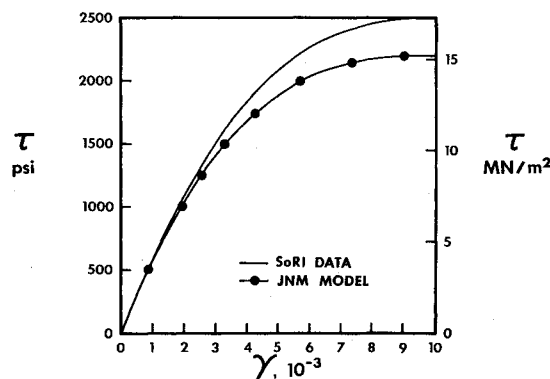


Fig. 17 Shear stress-strain behavior in x-y plane.

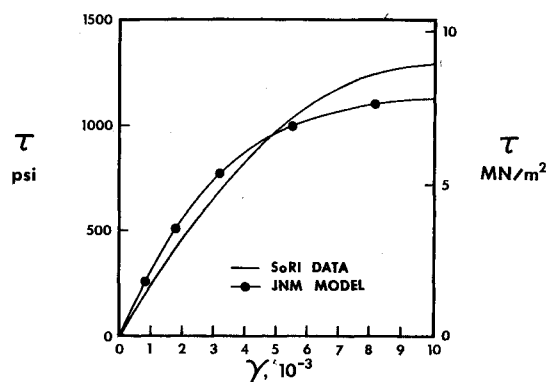


Fig. 18 Shear stress-strain behavior in x-z plane.

the measured response to be closer to the z direction response than occurs. A similar set of curves is shown for the x-z plane compression behavior in Fig. 16. There, the predicted response at 22½ deg to the x direction is below the measured response. The predicted 22½ deg response does not rise significantly when the z direction behavior is modeled as a continuously rising curve, instead of the broken curve in Fig. 16. That is, even if we ignore whatever physical reason that causes the broken curve and assume it will not happen in off-axis loading, we do not obtain a higher 22xz predicted response.

The measured and predicted x-y plane shear response is shown in Fig. 17. There, we see that the predicted response is somewhat below the measured response. For the x-z plane in Fig. 18, the predicted response is first higher and then lower than the measured response. In both cases, the predicted response is reasonably close to the measured response, especially when we consider the imperfect nature of the shear test.<sup>10</sup>

### Concluding Remarks

The class of fiber-reinforced composite materials called carbon-carbon is investigated from the standpoint of mechanical response to loading. This class has many characteristics that require modeling and analysis techniques of a complexity well beyond those used for simpler materials. A specific material model is developed for a representative carbon-carbon, namely AVCO Mod 3a, a rectangularly orthotropic material. Next, a single response measurement, the uniaxial off-axis loading test, is discussed from the standpoint of how to account for the shear coupling, which for orthotropic materials is inherent to that test. A method for adjusting predicted strain response to account for the shear coupling is developed. Then, strain response predictions for off-axis loading in two planes of AVCO Mod 3a carbon-carbon are compared with measured response. The response predictions are quite reasonable when we consider the fact

that stress-strain data used to define the Jones-Nelson-Morgan model are based on "most probable value" curves. "Most probable value" curves are an approximate, but statistically incomplete, representation of a collection of somewhat inconsistent and highly variable (from billet to billet) stress-strain curves. Thus, agreement between predicted and measured response is no guarantee of material model validity nor is disagreement necessarily an indication of material model invalidity. However, the Jones-Nelson-Morgan nonlinear multimodulus material model appears to be a reasonable representation of carbon-carbon behavior, although the model must be validated for more complex strain response than the present uniaxial off-axis loading test. Other possible material model validation tests are discussed by Jones.<sup>9</sup>

### Acknowledgment

This research was supported by the Air Force Office of Scientific Research/NA, Air Force Systems Command, USAF, under AFOSR Grant 73-2532. The understanding and patience of W. J. Walker, formerly of AFOSR (now of the Boeing Aerospace Company), during this investigation is sincerely appreciated.

### References

<sup>1</sup>Jones, R. M. and Nelson, D.A.R., Jr., "Material Models for Nonlinear Deformation of Graphite," *AIAA Journal*, Vol. 14, June 1976, pp. 706-717.

<sup>2</sup>Jones, R. M. and Nelson, D.A.R., Jr., "Theoretical-Experimental Correlation of Material Models for Nonlinear Deformation of Graphite," *AIAA Journal*, Vol. 14, Oct. 1976, pp. 1427-1435.

<sup>3</sup>Jones, R. M. and Morgan, H. S., "Analysis of Nonlinear Stress-Strain Behavior of Fiber-Reinforced Composite Materials," *AIAA Journal*, Vol. 15, Dec. 1977, pp. 1669-1676.

<sup>4</sup>Starrett, H. S., Weiler, F. C., and Pears, C. D., "Thermostructural Response of Carbon-Carbon Materials Under High Heat Flux Environments," Southern Research Inst., Birmingham, Ala., Air Force Materials Laboratory, Tech. Rept. AFML-TR-74-232, June 1975.

<sup>5</sup>Jones, R. M., "JNMDATA, A Preprocessor Computer Program for the Jones-Nelson-Morgan Nonlinear Material Models," Informal AFOSR Report, Civil and Mechanical Engineering Dept., Southern Methodist Univ., Dallas, Tex., April 1977.

<sup>6</sup>Starrett, H. S. and Pears, C. D., "Elastic Compliances for ATJ-S Graphite and Mod 3a Carbon-Carbon," Southern Research Inst., Birmingham, Ala., Air Force Materials Laboratory, Tech. Rept. AFML-TR-74-271, Feb. 1975.

<sup>7</sup>Pagano, N. J. and Halpin, J. C., "Influence of End Constraint in the Testing of Anisotropic Bodies," *Journal of Composite Materials*, Jan. 1968, pp. 18-31.

<sup>8</sup>Jones, R. M., *Mechanics of Composite Materials*, McGraw-Hill Book Co., Inc., New York, 1975.

<sup>9</sup>Jones, R. M., "Mechanics of Composite Materials with Different Moduli in Tension and Compression," AFOSR-TR-78-1400, CME Dept., Southern Methodist University, Dallas, Tex., July 1978.

<sup>10</sup>Iosipescu, N., "New Accurate Procedure for Single Shear Testing of Metals," *Journal of Materials*, Sept. 1967, pp. 537-566.

## *From the AIAA Progress in Astronautics and Aeronautics Series*

# SPACE SYSTEMS AND THEIR INTERACTIONS WITH EARTH'S SPACE ENVIRONMENT—v. 71

*Edited by Henry B. Garrett and Charles P. Pike, Air Force Geophysics Laboratory*

This volume presents a wide-ranging scientific examination of the many aspects of the interaction between space systems and the space environment, a subject of growing importance in view of the ever more complicated missions to be performed in space and in view of the ever growing intricacy of spacecraft systems. Among the many fascinating topics are such matters as: the changes in the upper atmosphere, in the ionosphere, in the plasmasphere, and in the magnetosphere, due to vapor or gas releases from large space vehicles; electrical charging of the spacecraft by action of solar radiation and by interaction with the ionosphere, and the subsequent effects of such accumulation; the effects of microwave beams on the ionosphere, including not only radiative heating but also electric breakdown of the surrounding gas; the creation of ionosphere "holes" and wakes by rapidly moving spacecraft; the occurrence of arcs and the effects of such arcing in orbital spacecraft; the effects on space systems of the radiation environment, etc. Included are discussions of the details of the space environment itself, e.g., the characteristics of the upper atmosphere and of the outer atmosphere at great distances from the Earth; and the diverse physical radiations prevalent in outer space, especially in Earth's magnetosphere. A subject as diverse as this necessarily is an interdisciplinary one. It is therefore expected that this volume, based mainly on invited papers, will prove of value.

737 pp., 6 × 9, illus., \$30.00 Mem., \$55.00 List

TO ORDER WRITE: Publications Dept., AIAA, 1290 Avenue of the Americas, New York, N.Y. 10104